Regular Article

PHYSICAL CHEMISTRY RESEARCH
Published by the
Iranian Chemical Society
www.physchemres.org
info@physchemres.org

Phys. Chem. Res., Vol. 11, No. 1, 171-180, March 2023
DOI: 10.22036/PCR.2022.333195.2048

Removal of Pb(II) Ion from Aqueous Solution Using As-synthesized CuO/Cu_2O Nanocomposites

M. Jarosova[a,*], S.A. Abed[b], P. Machek[a], R. Solanki[c], F.H. Alsultany[d], A.D. Khalaji[e,*] and S.A. Hussein[f,*]

[a]*Institute of Physic of the Czech Academy of Sciences, v.v.i., Na Slovance 2, 182 21 Prague 8, Czech Republic*
[b]*College of Science, University of Al-Al-Qadisiyah, Iraq*
[c]*Ph.D. Scholar Research, Scholar Department of Chemistry, Dr. A.P.J. Abdul Kalam University Indore India*
[d]*Medical Physics Department, Al-Mustaqbal University College, 51001 Hillah, Babil, Iraq*
[e]*Department of Chemistry, Faculty of Science, Golestan University, Gorgan, Iran*
[f]*Al-Manara College for Medical Sciences, Maysan, Iraq*
(Received 8 March 2022, Accepted 23 May 2022)

In this paper, the spherical CuO/Cu_2O nanocomposites were synthesized using co-precipitation accompanied by annealing at 500 and 600 ºC. The as-synthesized CuO/Cu_2O nanocomposites were characterized by Fourier transform infrared (FT-IR) spectroscopy, X-ray diffraction (XRD) and transmission electron microscope (TEM). The XRD and FT-IR results proved the successful synthesis of the CuO/Cu_2O nanocomposite. Spherical shapes of the samples confirmed by the TEM images with narrow particle size distribution. The average size of the nanocomposites synthesized at 600 °C (39 nm) was smaller than that of the nanocomposites synthesized at 500 °C (46 nm). In addition, the samples were chemically activated using H_2O_2 and used as new adsorbents to remove the Pb(II) ion from an aqueous solution. The effect of solution pH, sorbent dose, initial Pb(II) concentration, and the contact time were studied. Results showed that the highest efficiency (85% for the nanocomposites synthesized at 500 °C and 92% for the nanocomposites synthesized at 600 °C) was obtained at pH 6, 90 min contact time, 30 ppm Pb(II) solution, and 0.02 g of the sorbent. The Pb(II) adsorption equilibrium data were fitted well to the Langmuir model.

Keywords: CuO/Cu_2O nanocomposites, Co-precipitation, Adsorbent, Pb(II) Removal, Langmuir

INTRODUCTION

Nowadays, water pollution caused by toxic and dangerous organic dyes [1,2] and heavy metal ions [3,4] is one of the most important challenges all around the world. The presence of toxic heavy metal ions in water has adverse effects on animals, plants, and even humans. They are stable in the nature and do not disappear easily and quickly. Therefore, it is necessary to remove these ions from wastewater before discharging into environment; this is one of the most important goals of chemical engineering [5-8]. To do so, several methods have been reported such as chemical precipitation, ion-exchange, adsorption, membrane filtration, coagulation–flocculation, flotation, and electrochemical [9,10]. Among these methods, the adsorption process is the most popular one due to its simplicity and high efficiency. Also, it does not require complex and expensive equipment [7,8,11,12]. However, the choice of adsorbent type plays an important role in this method [7,8,11,12]. Recently, the application of transition metal oxide nanoparticles for the adsorption and removal of heavy metal ions, due to their large surface area and availability, has been an interesting area of research [3,5,6].

*Corresponding authors. E-mail: jarosova@fzu.cz; shaimaa2021@uomanara.edu.iq; alidkhalaji@yahoo.com

Among them, the copper oxides (CuO and Cu_2O) have attracted attention due to their properties (narrow band gap as p-type semiconductors) and their practical applications [13-15]. In recent years, many articles have been reported on the use of copper oxide nanoparticles for removal of metal ions [16,17]. For example, Raul et al. used copper oxide nanorods to remove Pb(II) ions from an aqueous solution. The study revealed that 92% of Pb(II) ions was removed in 60 min using this adsorbent [18]. Din Mahmoud *et al*. [16] used copper oxide nanoparticles synthesized by green chemistry to remove Pb(II), Ni(II) and Cd(II) ions. Their results showed that the removal efficiency of Pb(II) ions was higher than that of Ni(II) and Cd(II) ions.

Continuing the previous work on the preparation of various transition metal nanoparticles [19-21], the main purpose of this paper is to prepare CuO/Cu_2O nanocomposites and use them as efficient adsorbents to remove Pb(II) ions from an aqueous solution.

EXPERIMENTAL

Materials and Methods

Copper(II) acetate mono hydrate, oxalic acid, and lead(II) nitrate were purchased from Merck Company and used without further purification. FT-IR was recorded using a Perkin-Elmer spectrophotometer from 4000 to 400 cm^{-1}. The XRD patterns were obtained on Empyrean powder diffractometer of PANalytical in the range 2θ = 10-80° (Cu Kα radiation, λ = 1.5418 Å). TEM images were obtained by transmission electron microscope Philips CM120 with LaB_6 cathode operating at 120 kV and equipped with CCD camera Olympus Veleta.

Preparation of CuO/Cu_2O Nanocomposites

3 g of $Cu(CH_3COO)_2{\cdot}H_2O$ and 3 g oxalic acid were poured into a beaker containing 20 ml of water and stirred for 3 h. The final mixture was completely dried at 90 °C for 6 h. After that, the resulting precipitate was ground in a crucible and annealed in the electric furnace at 500 and 600 °C for 3 h. The resulting black precipitates were washed with distilled water, filtered, dried under ambient atmosphere, and characterized by FT-IR, XRD and TEM.

Removal of Pb(II) Ion

Solutions with concentrations of 10, 30, 50, 70, 90, and 110 ppm were prepared by dissolving lead nitrate in distilled water. In order to predict the adsorption behavior, a series of experiments were conducted as a function of contact time, initial Pb(II) concentration, pH solution, and sorbent dose. Sample in a 100 ml Erlenmeyer flask containing 50 ml of the Pb(II) solution were continuously stirred in an air bath shaker at 200 rpm and constant temperature of 30 for certain times varying from 0 to 120 min. In order to produce an activated sorbents, about 2 ml of H_2O_2 was added to the suspension. The solution pH was adjusted as needed using HCl (0.1 M) or NaOH (0.1 M). Then, at different stirring times, after removing adsorbent by centrifuge, the concentration of Pb(II) ions was measured using atomic adsorption. All the experiments were replicated three times. The Pb(II) removal efficiency (%) and adsorption capacity (mg g^{-1}) were calculated using the following formulas:

$$R\ (\%) = \{(C_o - C_t)/C_o\} \times 100 \quad (1)$$

$$q\ (mg\ g^{-1}) = \{(C_o - C_t)/M\} \times V \quad (2)$$

Here, C_o and C_t are the initial and final concentrations of Pb(II) ions in solution, respectively. V and M are the volume of the solution and the mass of the adsorbent, respectively.

The adsorption kinetic for the adsorption of Pb(II) ion onto as-prepared CuO/Cu_2O nanocomposites was studied by the two different models of pseudo-first and second-order models, and the equations are given below:

$$\ln(q_e - q_t) = \ln q_e - k_1 t \quad (3)$$

$$t/q_t = 1/k_2 q_e^2 + t/q_e \quad (4)$$

Here, k_1 (min^{-1}) and k_2 (g mg^{-1} min^{-1}) are the pseudo-first and second-order rate constant values. q_e and q_t (mg g^{-1}) are the adsorption capacity of as-prepared CuO/Cu_2O nanocomposites at equilibrium and at time t (min), respectively.

Lanmuir's and Freundlich isotherm models were generally studied to sorption mechanism of Pb(II) metal ions as-prepared CuO/Cu_2O nanocomposites and the equations are given below:

$$C_e/q_e = 1/q_t b + C_e/q_t \quad (5)$$

$$\ln q_e = \ln k_F + \ln C_e/n \quad (6)$$

Here, b (lmg^{-1}) and K_F are the Langmuir and Freundlich constants.

RESULTS AND DISCUSSION

Characterization of CuO/Cu_2O Nanocomposites

FT-IR, XRD and TEM techniques were used to characterize synthetic CuO/Cu_2O nanocomposites. Figure 1 shows the FT-IR spectra of the copper precursor and of the as-synthesized CuO/Cu_2O nanocomposites. In the FT-IR spectrum of the copper precursor, broad peaks, observed at 3423 and 1642 cm^{-1}, belong to the hydroxyl and carbonyl groups of the oxalic acid, respectively. The sharp peak at 489 cm^{-1} confirms the presence of Cu-O bonds in the compound. By thermal decomposition of the copper precursor at temperatures of 500 and 600 °C, the peaks of the oxalic acid group were removed. In the FT-IR spectrum of the as-synthesized CuO/Cu_2O nanocomposites, several peaks were obtained in the range of 480 to 620 cm^{-1} that are attributed to the vibrations of Cu^{I}-O and Cu^{II}-O bonds [21]. In these compounds, a weak and broad peak at 1620 cm^{-1} can be assigned to the moisture or water molecules adsorbed on the nanoparticles [21].

The XRD patterns of the as-synthesized CuO/Cu_2O nanocomposites are shown in Fig. 2. The peaks that appeared at the angles of 29.55°, 36.40°, 42.28°, 61.33°, and 73.46° can be assigned to the (110), (111), (200), (220), and (311) crystal planes of the cubic Cu_2O (ICSD 172174) [13-15]. The peaks appearing at the angles of 32.49°, 35.40°, 35.54°, 38.66°, 38.90°, 48.77°, 53.43°, 58.16°, 61.52°, 65.74°, 66.23°, 68.04°, 72.27°, 74.91°, and 75.24° correspond to the crystal planes (110), (002), (11-1), (111), (200), (20-2), (020), (202), (11-3), (022), (31-1), (220), (311), (004), and (22-2) of the monoclinic CuO (ICSD 291390) [13-15]. Moreover, there is one tiny impurity peak at 43.35° in the sample synthesized at 500 °C, which disappears at higher temperature. Otherwise, the sharpness and broadness of the peaks confirm good crystallinity and purity of the as-synthesized CuO/Cu_2O nanocomposites.

Rietveld fits revealed that CuO/Cu_2O nanocomposite

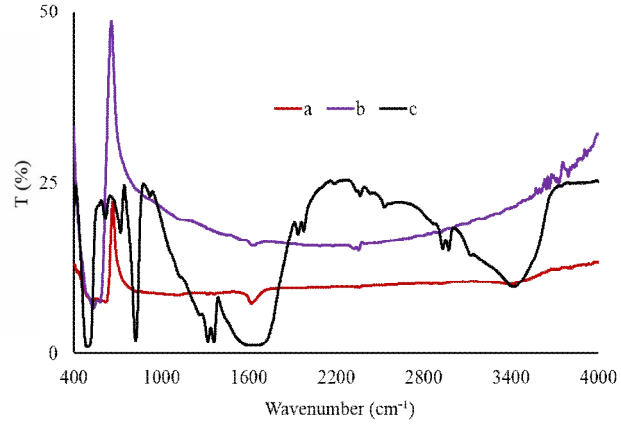

Fig. 1. FT-IR spectra of CuO/Cu_2O nanocomposites prepared at a) 500 °C, b) 600 °C and c) Cu precursor.

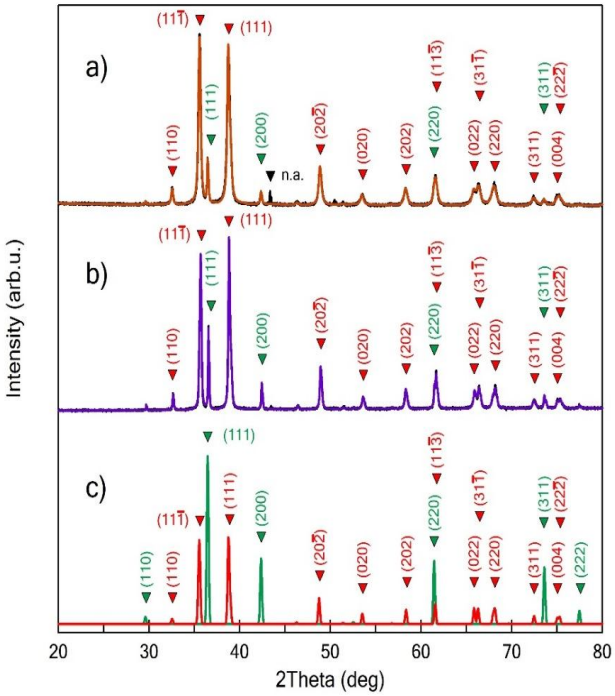

Fig. 2. XRD patterns of CuO/Cu_2O nanocomposites prepared at a) 500 °C and at b) 600 °C. Black dots represent measured points; color lines depict corresponding Rietveld fits. Green pattern in c) shows diffraction peaks of cubic Cu_2O (ICSD 172174), the red one diffraction peaks of monoclinic CuO (ICSD 291390).

Table 1. Structural Parameters of CuO/Cu_2O Nanocomposites Synthetized at 500 and 600 °C

	Temperature (°C)		500	600
Cu_2O	Fraction	(%)	7.5	14.8
(Pn-3m)	a	(Å)	4.2691(2)	4.2715(1)
	Fraction	(%)	92.5	85.2
CuO	a	(Å)	4.6851(2)	4.6887(1)
	b	(Å)	3.4280(2)	3.4264(1)
(C2/c)	c	(Å)	5.1313(2)	5.1346(1)
	β	(°)	99.378(2)	99.345(1)

synthesized at 500 °C consisted of 7.5 % cubic Cu_2O (space group 'Pn-3m') and 92.5 % monoclinic CuO phase (space group 'C2/c'); at higher temperature, the content of cubic Cu2O raised to 14.8 %. All structural parameters for the both samples are summarized in Table 1.

It is known that line broadening of diffraction peaks in the XRD patterns of samples is influenced by the average crystallite size [22]. The average crystallite size of as-synthesized nanocomposites can be calculated using Scherrer's equation [22]. It was about 39 nm for sample synthesized at 600 °C and about 46 nm for sample synthesized at 500 °C.

$$D = 0.94\lambda/\beta\cos\theta \quad (7)$$

Here, λ is the wavelength (0.154, CuKα), β is the full width at half maximum (FWHM), and θ is the diffraction angle. The two sharp peaks appeared at 2θ values of 35.6 and 38.8° were chosen to calculate the crystallite size of the as-synthesized nanocomposites.

The shape and the size of the as-prepared CuO/Cu_2O nanocomposites were examined by the TEM. Figure 3 shows the obtained TEM images. Despite the effort to separate individual particles in ultrasound, there were particle clusters in the figures. The particles had almost spherical or elliptical shapes. The size of the particles was in the ranges of several nanometers to low tens of nanometers. The average equivalent diameter was estimated to be approximately 20 nm. Accurate image analysis of the particle size distribution was not possible due to the enormous particle overlap in the clusters.

Pb(II) Removal Study

Important parameters such as pH, shaking time, adsorbent dose, and the initial concentration of heavy metal

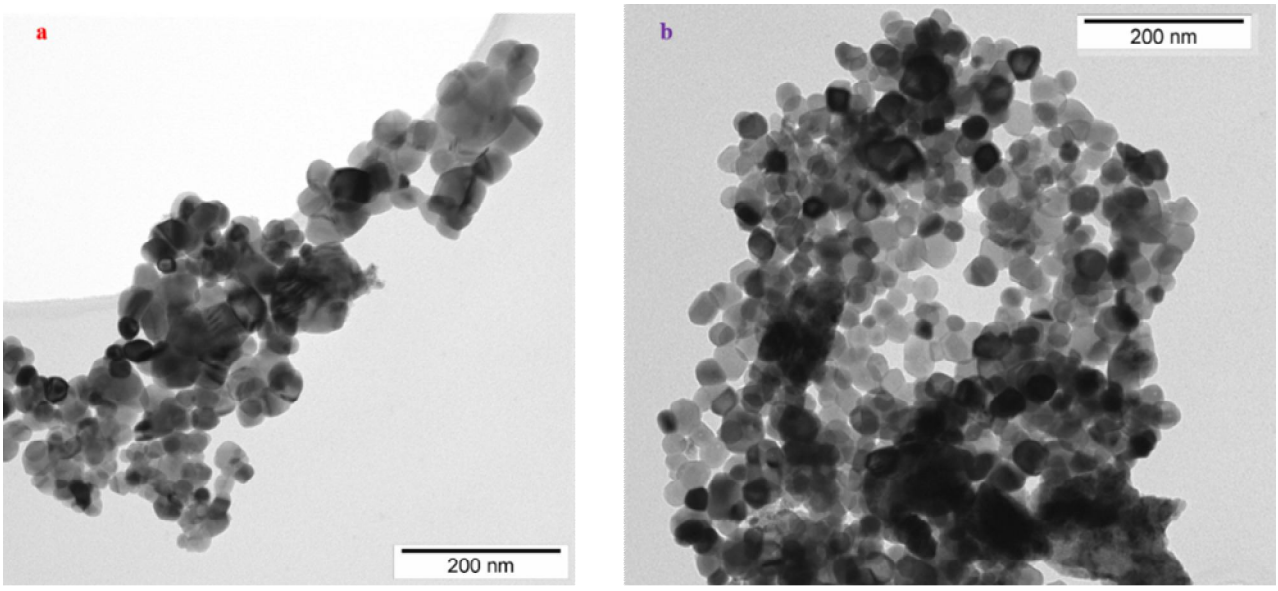

Fig. 3. TEM images of CuO/Cu_2O nanocomposites prepared at a) 500 °C and b) 600 °C.

ions can influence the removal percentage of heavy metal ions using various adsorbents [7-12,16,17]. At pHs < 4, the active groups on the surface of the adsorbent were protonated and could not be coordinated to the Pb(II) ions. Also, an electrostatic repulsion between the Pb(II) lead ions and the protonated groups on the surface of adsorbent caused low removal efficiency. However, at pHs > 7, the removal efficiency the Pb(II) ion was also low due to the precipitations of $Pb(OH)^{+}$ and $Pb(OH)_2$ [7-12,16,17]. Figure 4 shows the effect of pH on the removal of Pb(II) ions. It was observed that the maximum adsorptive removal of Pb(II) occurred at pH 6 [16,17].

The adsorbent dose is another important parameter [7-12]. Figure 5 shows the effect of adsorbent dose on the adsorption of Pb(II) ion using as-prepared CuO/Cu_2O nanocomposites at room temperature. It was obtained that the removal of Pb(II) was increased by an increases in adsorbent dose. This observance was due to an increase in active groups from 0.005 to 0.02 g; the removal percentage reached up to 85% for the CuO/Cu_2O prepared at 500 °C and 92% for the CuO/Cu_2O prepared at 600 °C. At low adsorbents dose, the active groups are fully coordinated by the Pb(II) ions. Therefore, large amount of Pb(II) ions cannot be coordinated to sorbent and remains in the solution [16,17]. The subsequent increase of the adsorbent dose does not cause any noticeable change in the absorption efficiency.

Figure 6 shows the effect of shaking time on the adsorption of Pb(II) ion. It was shown that in the first 15 min, the amount of Pb(II) ion removal was very intense. This is due to the high number of active groups in adsorbent and also the high concentration of Pb(II) ions. After that, due to the decrease in the amount of Pb(II) ions and also the active groups on the adsorbents, the removal of Pb(II) ions continued at a slower rate and reached its maximum value in 90 min [16,17].

Figure 7 shows the effect of initial concentration of Pb(II) ion on its removal efficiency by as-synthesized CuO/Cu_2O nanocomposites. The removal efficiency by the adsorbent decreased by an increase in the initial concentration of Pb(II) ions from 10 to 110 ppm. At low Pb(II) concentration (10 ppm), the better interaction of active groups on the adsorbent surface with Pb(II) ions and also the rapid and easy migration of the Pb(II) ion to the

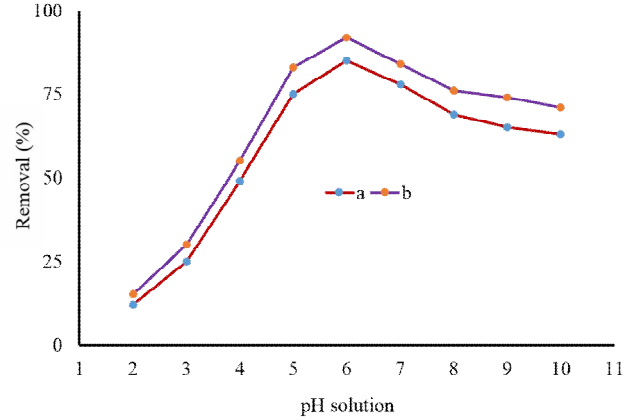

Fig. 4. Effect of pH on the Pb(II) removal using CuO/Cu_2O nanocomposites (Pb(II) concentration: 30 ppm, Shaking time: 90 min and adsorbent dose: 0.02 g).

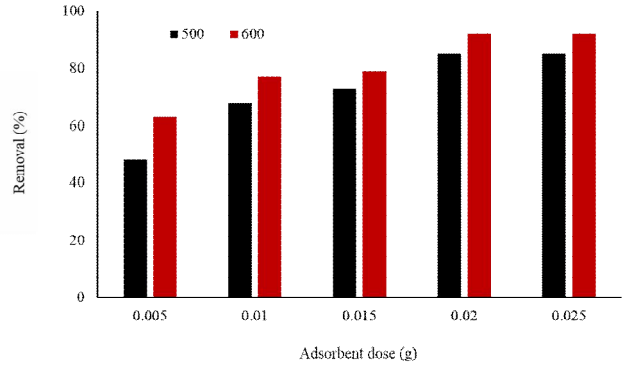

Fig. 5. Effect of sorbent dose on the Pb(II) removal using CuO/Cu_2O nanocomposites (Pb(II) concentration: 30 ppm, Shaking time: 90 min and pH solution: 6).

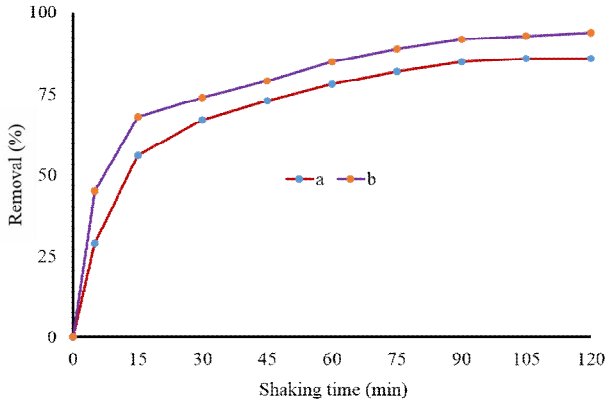

Fig. 6. Effect of shaking time on the Pb(II) removal using CuO/Cu_2O nanocomposites (Pb(II) concentration: 30 ppm, adsorbent dose: 0.02 g and pH solution: 6).

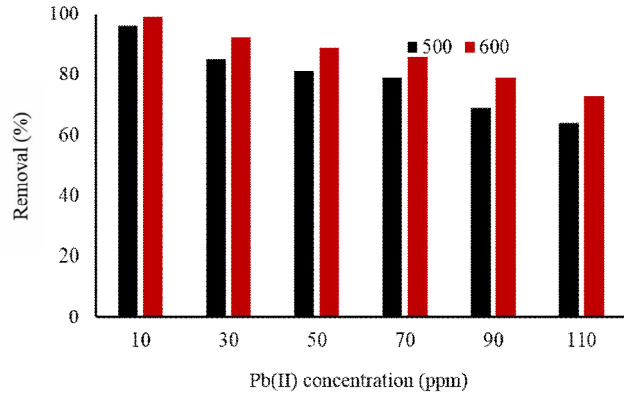

Fig. 7. Effect of initial Pb(II) concentration on the Pb(II) removal using CuO/Cu_2O nanocomposites (shaking time: 90 min, adsorbent dose: 0.02 g and pH solution: 6).

adsorbent surface resulted in a high efficient removal of the Pb(II) ion (96% for the sample prepared at 500 °C and 99% for the sample prepared at 600 °C) from aqueous solution. An increase in the concentration of the Pb(II) ions prevented some of the Pb(II) ions from interacting with the active site of sorbent (due to occupation of them by Pb(II) ion) [23-27]. In this case, some of the Pb(II) ions could not be removed from the environment [26,17]. Adsorption capacities of samples were calculated and they are shown in Table 2.

Table 3 represents the comparison of the adsorption capacity of other sorbents and as-prepared current CuO/Cu_2O nanocomposites for the Pb(II) ion. Results revealed that the as-prepared CuO/Cu_2O nanocomposites was a promising adsorbents for the removal of Pb(II) ion.

In the real water, there are different cations (Na^+, Ca^{2+}, Mg^{2+}) and anions (NO_3^-, Cl^-, PO_4^{3-}) that can affect the adsorption performance of the adsorbents [31-33]. The effect of these coexisting ions on the Pb(II) removal using as-synthesized CuO/Cu_2O nanocomposites were studied.

Adsorption Kinetics

Figures 8 and 9 represent the pseudo-first and second-order adsorption kinetics of Pb(II) ion onto the as-synthesized CuO/Cu_2O nanocomposites, respectively. By comparing the straight lines of the adsorption profiles, it can be seen that adsorption kinetics followed the pseudo

Table 2. Adsorption Capacities of As-prepared CuO/Cu_2O Nanocomposites

Pb(II) concentration		10	30	50	70	90	110
q (mg g^{-1})	CuO/Cu_2O Prepared at 500 °C	24.0	63.7	105.0	138.2	155.2	176
	CuO/Cu_2O Prepared at 600 °C	24.7	69.0	111.2	150.5	177.7	200.7

Table 3. A comparative of Adsorption Capacities for Pb(II) Using Various Adsorbents

Adsorbents	Adsorption capacity (mg g^{-1})	Ref.
CuO/Cu_2O	63.7 and 69	This work
CuO	37.02	[17]
CuO	88.8	[16]
Cu/Mg Binary ferrite	57.7	[23]
ECCSB@Fe_3O_4	86.2	[11]
m-CSPIB	104.16	[12]
NPCS-PEI	645.16	[28]
Sulfhydryl modified chitosan	273.7	[29]
Chitosan/lignosulfonate	525	[30]

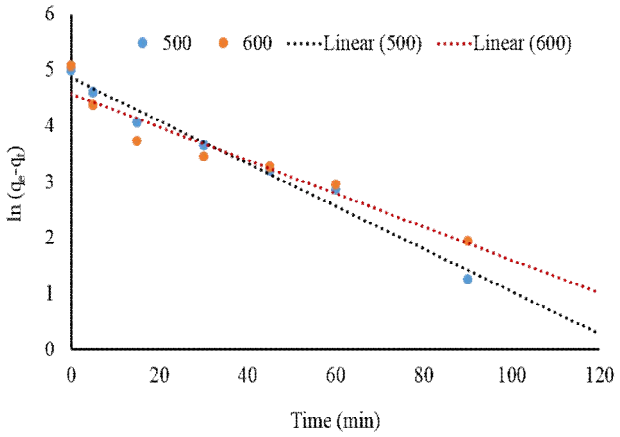

Fig. 8. Pseudo first-order equation curve for Pb(II) ion adsorption onto CuO/Cu_2O nanocomposites.

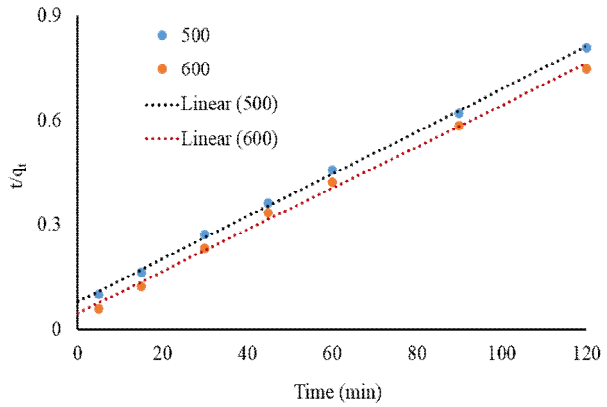

Fig. 9. Pseudo second-order equation curve for Pb(II) ion adsorption onto CuO/Cu_2O nanocomposites.

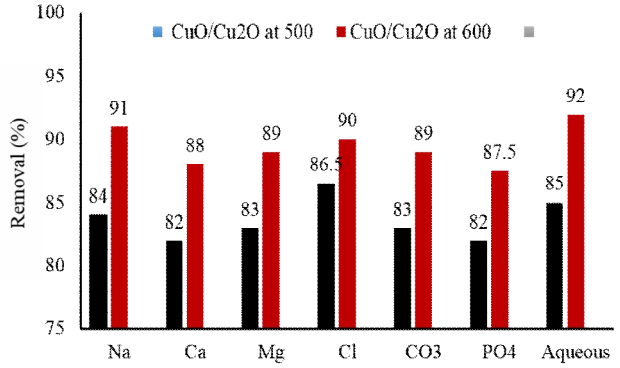

Fig. 8. The effect of coexisting ions on the Pb(II) removal using as-synthesized CuO/Cu_2O nanocomposites.

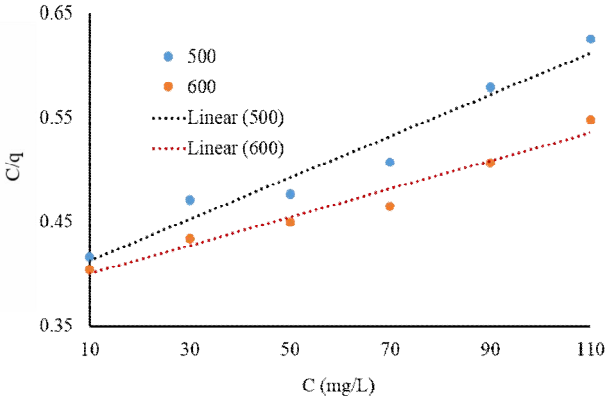

Fig. 10. Longmuir isotherm for Pb(II) ion adsorption onto CuO/Cu_2O nanocomposites.

second-order model [17,23,27], which confirmed that the adsorption capacity was related to the active sites on the surface of the as-synthesized CuO/Cu_2O nanocomposites.

Adsorption Isotherms

In order to investigate mechanism of Pb(II) ion adsorption onto the as-synthesized CuO/Cu_2O nanocomposites, the Langmuir and Freundlich isotherm were studied and the curves are given in Figs. 10 and 11, respectively. It was observed that the Freundlich isotherm was more suitable for adsorption of Pb(II) ion on the surface of the as-synthesized CuO/Cu_2O nanocomposites [34]. This indicates that the adsorption of Pb(II) ion was carried out by multiple and heterogeneous layers of the surface of the samples [35].

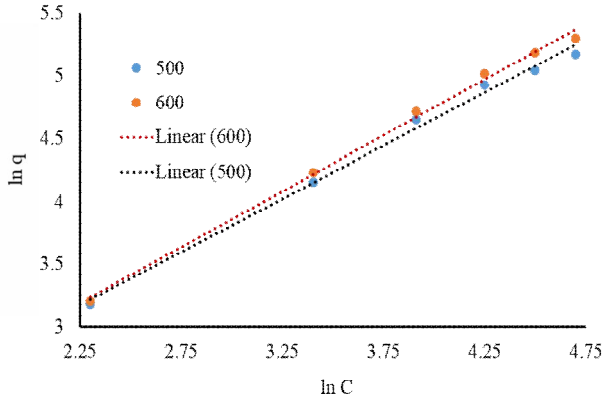

Fig. 11. Freundlich isotherm for Pb(II) ion adsorption onto CuO/Cu_2O nanocomposites

CONCLUSIONS

The pure CuO/Cu_2O nanocomposites were successfully synthesized using thermal decomposition at 500 and 600 °C as a facile and low-cost route. FT-IR and XRD patterns confirmed the preparation of pure and single crystalline phase of CuO/Cu_2O nanocomposites. The adsorption of Pb(II) using the as-prepared CuO/Cu_2O nanocomposites was found to be dependent on the pH solution, sorbent dose, shaking time, and the initial concentration of Pb(II). The maximum removal efficiencies of Pb(II) was 92% and 85% using samples at the optimum equilibrium contact time of 120 min, sorbent dose of 0.02 g, and initial Pb(II) concentration of 70 mg/L. The experimental data predicted that the Pb(II) adsorption followed the pseudo second-order, and the adsorption process was fitted to the Freundlich isotherm model.

ACKNOWLEDGMENTS

The work was supported by Operational Programme Research, Development and Education financed by European Structural and Investment Funds and the Czech Ministry of Education, Youth and Sports (Project No. SOLID21 CZ.02.1.01/0.0/0.0/16_019/0000760). SAA, RS, FHA, ADK and SAH would like to thank the University of Al-Al-Qadisiyah, Abdul Kalam University, Al-Mustaqbal University College, Golestan University and Al-Manara College for Medical Sciences for their financial supports.

CONFLICT OF INTEREST

The authors declare that they have no conflict of interest.

AUTHOR CONTRIBUTIONS

M. Jarosova and P. Machek gathered XRD patterns and TEM images. A.D. Khalaji prepared the samples and recorded FT-IR spectra. S.A. Abed, R. Solanki, F.H. Alsultany, and S. Abed Hussein prepared samples and investigated the photocatalytic activity of samples. A.D. Khalaji wrote the main manuscript. All authors reviewed and revised the MS.

REFERENCES

[1] Yazid, H.; Achour, Y.; El Kassimi, A.; Nadir, I.; El Himri, M.; Laamari, M.; El Haddad, M., Removal of congo red from aqueous solution using cuttlefish bone powder, *Phys. Chem. Res.* **2021**, *9*, 565-577. DOI: 10.22036/pcr.2021.278943.1901.

[2] Sharafinia, A.; Farrokhnia, A.; Ghasemian, E., Comparative study of adsorption of safranin o by TiO2/activated carbon and chitosan/TiO_2/activated carbon adsorbents, *Phys. Chem. Res.* **2021**, *9*, 605-621. DOI: 10.22036/PCR.2021.274568.1889.

[3] Tamez, C.; Hernandez, R.; Parsons, J. G., Removal of Cu(II) and Pb(II) from aqueous solution using engineerd iron oxide nanoparticles, *Microchim. J.* **2016**, *125*, 97-104. DOI: 10.1016/j.microc.2015.10.028.

[4] Kamatchi, C. I.; Arivoli, S.; Prabakaran, R., Thermodynamic, kinetic, batch adsorption and isotherm models for the adsorption of nickel from an artificial solution using chloroxylon swietenia activated carbon, *Phys. Chem. Res.* **2022**, *10*, 315-324. DOI: 10.22036/PCR.2021.300561.1956.

[5] Jerin, V. M.; Remya, R.; Thomas, M.; Vakey, J. T., Investigation on the removal of toxic chromium ion from waste water using Fe_2O_3 nanoparticles, *Mater. Today: Proceed.* **2019**, *9*, 27-31. DOI: 10.1016/j.matpr.2019.02.032.

[6] Cao, C. Y.; Qu, J.; Yan, W. S.; Zhu, J. F.; Wu, Z. Y.; Song, W. G., Low-cost synthesis of flowerlike α-Fe_2O_3 nanostructures for heavy metal ion removal: adsorption property and mechanism, *Langmuir* **2012**, *28*, 4573-4579. DOI: 10.1021/la300097y.

[7] Gu, F.; Geng, J.; Li, M.; Chang, J.; Dui, Y., Synthesis of chitosan-lignosulfonate composite as an adsorbent for dyes and metal ions removal from wastewater, *ACS Omega* **2019**, *4*, 21421-21430. DOI: 10.1021/acsomega.9b03128.

[8] Mousavi, S. M.; Hashemi, S. A.; Amani, A. M.; Esmaeili, H.; Ghasemi, Y.; Babapoor; Fatemeh Mojoudi, A.; Arjomand, O., Pb(II) removal from synthetic wastewater using kombucha scoby and graphene oxide/Fe_3O_4, *Phys. Chem. Res.* **2018**, *6*, 759-771. DOI: 10.22036/pcr.2018.133392.1490.

[9] Fu, F.; Wang, Q., Removal of heavy metal ions from

wastewaters: A review, *J. Environ. Manag.* **2011**, *92*, 407-418. DOI: 10.1016/j.jenvman.2010.11.011.

[10] Fato, F. P.; Li, D. W.; Zhao, L. J.; Qiu, K.; Long, Y. T., Simultaneous removal of multiple heavy metal ions from river water using ultrafine mesoporous magnetite nanoparticles, *ACS Omega* **2018**, *4*, 7543-7549. DOI: 10.1021/acsomega.9b00731.

[11] Yan, Y.; Yuvaraja, G.; Liu, C.; Kong, L.; Guo, K.; Reddy, G. M.; Zyryanov, G. V., Removal of Pb(II) ions from aqueous media using epichlorohydrin crosslinked chitosan Schiff's base@Fe_3O_4 (ECCSB@Fe_3O_4), *Int. J. Biol. Macromol.* **2018**, *117*, 1305-1313. DOI: 10.1016/j.ijbiomac.2018.05.204.

[12] Yuvaraj, G.; Subbaiah, M. V., Removal of Pb(II) ion by using magnetic chitosan-4-((pyridine-2-ylimino), ethyl)benzaldehyde Schiff's base, *Int. J. Biol. Macromol.* **2016**, *93*, 408-417. DOI: 10.1016/j.ijbiomac.2016.08.084.

[13] Yu, S. Y.; Gao, Y.; Chen, F. Z.; Fan, G. C.; Han, D. M.; Wang, C.; Zhao, W. W., Fast electrochemical deposition of CuO/Cu_2O heterojunction photoelectrode: preparation and application for rapid cathodic photoelectrochemical detection of L-cysteine, *Sens. Act. B. Chem.* **2019**, *290*, 312-317. DOI: 10.1016/j.snb.2019.03.104.

[14] Lv, J.; Kong, C.; Xu, Y.; Yang, Z.; Zhang, X.; Yang, S.; Meng, G.; Bi, J.; Li, J.; Yang, S., Facile synthesis of novel CuO/Cu_2O nanosheets on copper foil for high sensitive nonenzymatic glucose biosensor, *Sens. Act. B. Chem.* **2017**, *248*, 630-638. DOI: 10.1016/j.snb.2017.04.052.

[15] Zhang, L.; Cui, Z.; Wu, Q.; Guo, F.; Xu, Y.; Guo, L., Cu_2O-CuO composite microframes with well-designed micro/nano structures fabricated *via* controllable etching of Cu_2O microcubes for CO gas sensors, *Cryst. Eng. Commun.* **2013**, *15*, 7462-7467. DOI: 10.1039/C3CE40595H.

[16] Din Mahmoud, A. E.; Al-Qahtani, K. M.; Alflaii, S. O.; Al-Gahtani, S. F.; Alsamhan, F. A., Green copper oxide nanoparticles for lead, nickel, and cadmium removal from contaminated water, *Sci. Rep.* **2021**, *11*, 12547. DOI: 10.1038/s41598-021-91093-7.

[17] Verma, M.; Tyagi, I.; Chandra, R.; Gupta, V. K., Adsorptive removal of Pb(II) ions from aqueous solution using CuO nanoparticles synthesized by sputtering method, *J. Mol. Liq.* **2017**, *225*, 936-944. DOI: 10.1016/j.molliq.2016.04.045.

[18] Raul, P. K.; Senapati, S.; Sahoo, A. K.; Umlong, I. M.; Devi, R. R.; Thakur, A. J.; Veer, V., CuO nanorods: a potential and efficient adsorbent in water purification, *RSC Adv.* **2014**, *4*, 40580-40587. DOI: 10.1039/C4RA04619F.

[19] Khalaji, A. D.; Palang Sangdevini, Z.; Mousvi, S. M.; Jarosova, M.; Machek, P., Benzoic acid-functionalized α-Fe_2O_3 nanoparticles: synthesis, characterization, magnetic and optical properties, *Asian J. Nanosci., Mater.* **2021**, *4*, 137-146. DOI: 10.26655/AJNANOMAT.2021.2.4

[20] Khalaji, A. D.; Ghorbani, M.; Peyghoun, S. J.; Feizi, N.; Akbari, A.; Hornfeck, W.; Dusek, M.; Eigner, V., Vanadium(IV) Schiff base complex: Synthesis, characterization, crystal structure and thermal decomposition into V_2O_5 particles, *Chem. Method.* **2019**, *3*, 707-714. DOI: 10.33945/SAMI/CHEMM.2019.6.3.

[21] Khalaji, A.D.; Ghorbani, M.; Dusek, M.; Eigner, V., The Bis(4-methoxy-2-hydroxybenzophenone) copper(II) Complex Used as a New Precursor for Preparation of CuO Nanoparticles, *Chem. Method.* **2020**, *4*, 143-151. DOI: 10.33945/SAMI/CHEMM.2020.2.4

[22] Lassoued, A.; Lassoued, M. S.; Dkhil, B.; Ammar, S.; Gadri, A., Photocatalytic degradation of methyl orange dye by $NiFe_2O_4$ nanoparicles under visible irradiation: effect of varying the synthesis temperature, *J. Mater. Sci. Mater. Electron.* **2018**, *29*, 7057-7067. DOI: 10.1007/s10854-018-8693-0.

[23] Van Tran, C.; Viet Quang, D.; Nguyen Thi, H.P.; Trung, T.N.; Duc La, D., Effective Removal of Pb(II) from Aqueous Media by a New Design of Cu-Mg Binary Ferrite, *ACS Omega* **2020**, *5*, 7298-7306. DOI: 10.1021/acsomega.9b04126.

[24] Kaur, M.; Kumari, S.; Sharma, P., Removal of Pb(II) from aqueous solution using nanoadsorbent of Oryza sativa husk: Isotherm, kinetic and thermodynamic studies, *Biotechnol. Rep.* **2020**, *25*, e00410. DOI: 10.1016/j.btre.2019.e00410.

[25] Barrak, H.; Kriaa, A.; Triki, M.; Nif, A. M.; Hamzaoui,

A. H., Study of the adsorption and desorption of Zn(II) and Pb(II) on CaF_2 nanoparticles, *Iran. J. Chem. Chem. Eng.* **2020**, *39*, 191-201. DOI: 10.30492/IJCCE.2020.96636.3345.

[26] Ossman, M. E.; Abdelfattah, M., CuO nanopowder for removal of Pb(II) and Zn(II), *J. Environ. Eng. Sci.* **2015**, *10*, 10-18. DOI: 10.1680/jees.14.00013.

[27] Xu, P.; Zeng, G. M.; Huang, D. L.; Lai, C.; Zhao, M. H.; Wei, Z.; Li, N. J.; Huang, C.; Xie, G. X., Adsorption of Pb(II) by iron oxide nanoparticles immobilized phanerochaete chrysosporium: equilibrium, kinetic, thermodynamic and mechanisms analysis, *Chem. Eng. J.* **2012**, *203*, 423-431. DOI: 10.1016/j.cej.2012.07.048.

[28] Liu, T.; Gou, S.; He, Y.; Fang, S.; Zhou, L.; Gou, G.; Liu, L., N-methylene phosphonic chitosan aerogels for efficient capture of Cu^{2+} and Pb^{2+} from aqueous environment, *Carbohydr. Polym.* **2021**,*269*, 118355. DOI: 10.1016/j.carbpol.2021.118355.

[29] Yang, Y.; Zeng, L.; Lin, Z.; Jiang, H.; Zhang, A., Adsorption of Pb^{2+}, Cu^{2+}, and Cd^{2+} by sulfhydryl modified chitosan beads, *Carbohydr. Polym.* **2021**, *274*, 118622. DOI: 10.1016/j.carbpol.2021.118622.

[30] Zhang, F.; Wang, B.; Jie, P.; Zhu, J.; Cheng, F., Preparation of chitosan/lignosulfonate for effectively removing Pb(II), *Polymer* **2021**, *228*, 123878. DOI: 10.1016/j.polymer.2021.123878.

[31] Zhu, K.; Chen, C.; Wang, H.; Xie, Y.; Wakeel, M.; Wahid, A.; Zhang, X., Gamma-ferric oxide nanoparticles decoration onto porous layered double oxide belts for efficient removal of uranyl, *J. Colloid Interface Sci.* **2019**, *535*, 262-275. DOI: 10.1016/j.jcis.2018.10.005.

[32] Hao, H.; Liu, G.; Wang, Y.; Shi, B.; Han, K.; Zhuang, Y.; Kong, Y., Simultaneous cationic Cu(II) anionic Sb(III) removal by NH_2-Fe_3O_4-NTA core-shell magnetic nanoparticles sorbents synthesized *via* a facile one-pot approach, *J. Hazard. Mater.* **2019**, *362*, 246-257. DOI: 10.1016/j.jhazmat.2018.08.096.

[33] Zhao, W.; Ren, B.; Hursthouse, A.; Wang, Z., Facile synthesis of nanosheet-assembled γ-Fe_2O_3 magnetic microspheres and enhanced Sb(III) removal, *Environ. Sci. Poll. Res.* **2021**, *28*, 19822-19837. DOI: 10.1007/s11356-020-11727-7.

[34] Shariati, T.; Mehrdadi, N.; Tahmasebi, M., Study of cadmium and nickel removal from battery industry wastewater by Fe_2O_3 nanoparticles, *Pollution* **2019**, *5*, 515-524. DOI: 10.22059/POLL.2018.268193.530.

[35] Tamez, C.; Hernandez, R.; Parsons, J. G., Removal of Cu(II) and Pb(II) from aqueous solution using engineerd iron oxide nanoparticles, *Microchim. J.* **2016**, *125*, 97-104. DOI: 10.1016/j.microc.2015.10.028.